

Spin-charge-lattice coupling through resonant multimagnon excitations in multiferroic BiFeO₃

M. O. Ramirez,^{1,a)} A. Kumar,¹ S. A. Denev,¹ Y. H. Chu,^{2,3} J. Seidel,^{2,3} L. W. Martin,² S.-Y. Yang,² R. C. Rai,⁴ X. S. Xue,⁴ J. F. Ihlefeld,^{1,2} N. J. Podraza,¹ E. Saiz,² S. Lee,⁵ J. Klug,^{6,7} S. W. Cheong,⁵ M. J. Bedzyk,^{6,7} O. Auciello,⁷ D. G. Schlom,¹ J. Orenstein,³ R. Ramesh,^{2,3} J. L. Musfeldt,⁴ A. P. Litvinchuk,⁸ and V. Gopalan¹

¹Department of Materials Science and Engineering and Materials Research Institute, Pennsylvania State University, University Park, Pennsylvania 16802, USA

²Materials Sciences Division, Lawrence Berkeley National Laboratory, Berkeley, California 94720, USA

³Department of Physics, University of California, Berkeley, California 94720-1760, USA

⁴Department of Chemistry, University of Tennessee, Knoxville, Tennessee 37996, USA

⁵Department of Physics and Astronomy Rutgers Center of Emergent Materials, Rutgers, The State University of New Jersey, 136 Frelinghuysen Road, Piscataway, New Jersey 08854-8019, USA

⁶Materials Research Center, Northwestern University, Evanston, Illinois 60208, USA

⁷Materials Science Division, Argonne National Laboratory, Argonne, Illinois 60439, USA

⁸Department of Physics and Texas Center for Superconductivity and Advanced Materials, University of Houston, Houston, Texas 77204-5002, USA

(Received 27 December 2008; accepted 24 March 2009; published online 21 April 2009)

Spin-charge-lattice coupling mediated by multimagnon processes is demonstrated in multiferroic BiFeO₃. Experimental evidence of two- and three-magnon excitations as well as multimagnon coupling at electronic energy scales and high temperatures are reported. Temperature dependent Raman experiments show up to five resonant enhancements of the two-magnon excitation below the Néel temperature. These are shown to be collective interactions between on-site Fe *d-d* electronic resonance, phonons, and multimagnons. © 2009 American Institute of Physics.

[DOI: [10.1063/1.3118576](https://doi.org/10.1063/1.3118576)]

Spin-charge-lattice coupling is central to the current interest in multiferroic materials. In particular, the coupling between magnetization and polarization can lead to cross-coupled phenomena such as magnetic control of polarization and electrical control of magnetism.^{1,2} Multiferroic materials with both polar and magnetic order parameters usually show a relatively low-symmetry crystal structure due to the absence of both time and space inversion symmetries; hence, a strong interaction between the low-lying magnetic and lattice excitations can occur, leading to rich new physics phenomena. One widely studied mechanism for spin-charge coupling is through electromagnons, which are single-magnon spin waves that are excited by an ac electric field.³⁻⁶ A relatively unexplored mechanism in multiferroics is through multimagnon excitations, which are known to be very sensitive to temperature effects and phase transitions.⁷

Bismuth ferrite, BiFeO₃, the focus of this study, has a robust ferroelectric polarization ($\sim 100 \mu\text{C}/\text{cm}^2$) at room temperature (RT),⁸ that is the largest among known ferroelectrics. At RT, BiFeO₃ is a rhombohedrally distorted ferroelectric perovskite with space group *R3c* and a Curie temperature, $T_C < 1100 \text{ K}$.⁹ It also shows a *G*-type canted antiferromagnetic order below Néel temperature, $T_N < 640 \text{ K}$, and, in the bulk, an incommensurately space-modulated spin structure along (110)_{*h*}.¹⁰ During the past few years, various physical properties of BiFeO₃ have been reported to show anomalies across T_N .¹¹⁻¹⁴ However, with the exception of neutron diffraction, none of these properties, have cleanly distinguished the magnetism from the polar contribution in this material. This makes the study of coupled phenomena challenging. Here we show that combining

Raman scattering and linear optical spectroscopy of multimagnons, phonons, and electronic energy levels can reveal spin-charge-lattice coupling in this system.

For our experiments, 4.5 μm BiFeO₃ film on (110) DyScO₃ and BiFeO₃ single crystal were grown according to Refs. 12 and 14. The thick films were relaxed and had (001)_{*p*} pseudocube-on-pseudocube epitaxial geometry, with trigonal *C_{3v}* crystal structure. Raman spectra were recorded under excitation at 488 nm in a backscattering geometry by using a WITec alpha 300 S confocal Raman microscope equipped with a Linkam heating stage. Raman spectra were collected in unpolarized geometry. Optical transmittance measurements were performed using a Perkin Elmer Lambda-900 spectrometer between 4 and 730 K.

Though magnons energy are typically small ($< 100 \text{ cm}^{-1}$), Raman scattering for spin wave optical branches at higher energies have been previously reported in iron oxides due to their large unit cell, their corresponding multimagnon excitations located at energies larger than 1000 cm^{-1} .¹⁵ Figures 1(a) and 1(b) depict the high frequency unpolarized Raman spectra for a 4.5 μm thick epitaxial film of BiFeO₃ collected at different temperatures. Further details on the temperature dependent Raman spectra under 1300 cm^{-1} can be found in Refs. 11, 14, and 16. Evidence for two- and three-magnon scattering at the shoulder of a previously reported two-phonon overtone can be observed, their energy values peaking at ~ 1530 and 2350 cm^{-1} , respectively. The two- and three-magnon excitations were identified by using the striking spectral similarity between BiFeO₃ and $\alpha\text{-Fe}_2\text{O}_3$, the simplest case of an iron oxide containing only FeO₆ octahedra, where not only two-magnon scattering but also two-phonon overtones at very similar energies have been reported.^{14,15} (Our films and crystals were

^{a)}Electronic mail: mariola.ramirez@uam.es.

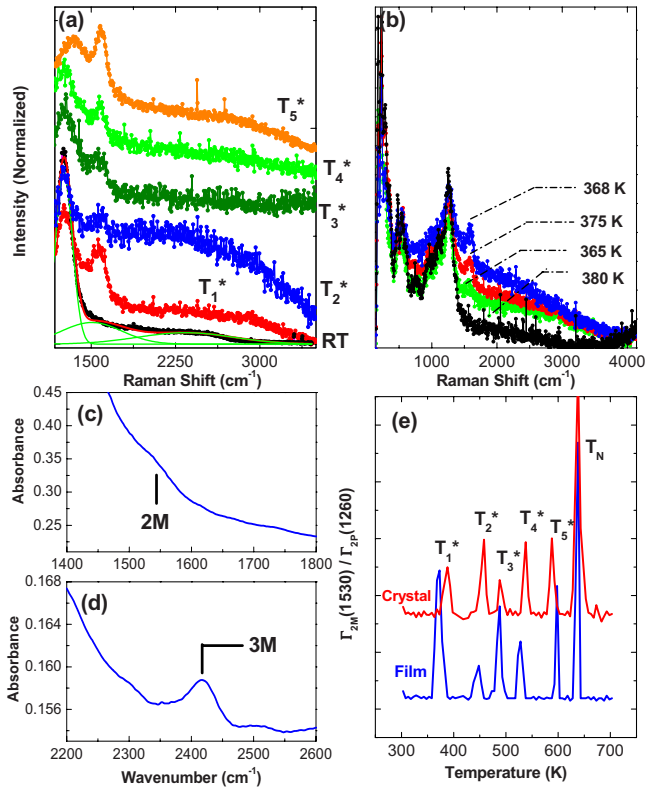


FIG. 1. (Color online) (a) Temperature-dependent Raman spectra of a $4.5 \mu\text{m}$ thick epitaxial BiFeO_3 film. The three Gaussian fits to RT spectra correspond to two-phonon, two-magnon, and three-magnon replica, respectively, from low-to-high wavenumber shift. For clarity, the spectra at $T_1^* = 365 \text{ K}$, $T_2^* = 450 \text{ K}$, $T_3^* = 490 \text{ K}$, $T_4^* = 530 \text{ K}$, and $T_5^* = 600 \text{ K}$, are normalized and vertically translated. (b) Evolution of the Raman spectra collected around T_1^* [(c) and (d)] RT midinfrared linear absorption measured on a BiFeO_3 bulk single crystal. (e) Integrated intensity ratio between the two-magnon and two-phonon Raman overtones as a function of temperature.

confirmed to be phase-pure BiFeO_3 by using synchrotron x-ray diffraction, transmission electron microscopy, and scanning probe microscopy). RT midinfrared absorption experiments were performed in the same spectral range [Figs. 1(c) and 1(d)]. The two-magnon absorption band can be seen around 1550 cm^{-1} [see Fig. 1(c)], though the strong contribution to the absorption spectra of the second order overtones in the $1400\text{--}1800 \text{ cm}^{-1}$ energy range precludes resolving this peak. At higher energies [Fig. 1(d)], an absorption band centered at $\sim 2415 \text{ cm}^{-1}$ is well resolved, which reasonably matches the three-magnon excitation from Raman scattering. These results not only support our previous assignments but also point out strong coupling interactions between the spin system (Fe-Fe exchange interaction) and electric dipole active excitations in BiFeO_3 .

Based on the position of the two magnon scattering observed in the Raman spectra, an estimate of the nearest neighbor exchange J , described by the Heisenberg Hamiltonian, can be made. If spin deviations are created on adjacent sites in a perovskite antiferromagnet, the excitation frequency of the system arising from two-magnon scattering is given by $J(2Sz-1)$, where S refers to the individual spin on the magnetic site and z represents the number of nearest neighbors to that site.⁷ In bismuth ferrite, the spin on Fe^{3+} site is $S = \frac{5}{2}$ and the number of nearest neighbors around Fe cation is $z = 6$. The frequency shift of the two magnon peak to the first approximation is given by $\omega(2M) = J(2Sz-1) = 29J$.

From experiments, the two magnon scattering peak is observed at 1530 cm^{-1} for BiFeO_3 in both film and crystal. Thus, the value of exchange interaction is obtained as $J \sim 1530/29 = 52.8 \text{ cm}^{-1} = 6.54 \text{ meV}$. This estimated value is in agreement with first principle calculations performed on BiFeO_3 using LDA+U method (for $U = 5 \text{ eV}$), where the $|J|$ value is estimated to be 7.4 meV .¹⁷

As the samples were heated, a striking enhancement of the two-magnon Raman bands was observed *only* within a $\sim 10 \text{ K}$ window around six different temperatures of $T_1^* = 365 \text{ K}$, $T_2^* = 450 \text{ K}$, $T_3^* = 490 \text{ K}$, $T_4^* = 530 \text{ K}$, $T_5^* = 600 \text{ K}$, and $T_N = 645 \text{ K}$, as seen from Figs. 1(a) and 1(e). Similar results were observed in single crystals. Unfortunately, the weak intensity and considerable linewidth of the two- and three-magnon excitations prevented a study of their temperature dependence in terms of frequency shift, broadening, and total intensity. Nonetheless, from the ratio between two-magnon ($< 1550 \text{ cm}^{-1}$) and two-phonon ($< 1260 \text{ cm}^{-1}$) excitations as a function of temperature, a clear plot of the temperature driven multimagnon enhancement can be obtained [Fig. 1(e)]. Since anomalies in the measured resistivity and induced magnetization were observed only at T_N , and not at any of T_1^* to T_5^* , it rules out spin reorientation transitions except at T_N . Also, a lack of any anomalous lattice parameter changes at these temperatures¹⁸ suggests that these are not structural phase transitions. We note that the two-phonon overtone—strongly enhanced due to the resonance with the intrinsic absorption edge—also couples strongly to T_N as shown previously.¹⁴ Hence, since the excitation energy ($E_{\text{exc}} < 2.54 \text{ eV}$) is close to the band edge, these anomalies appear to be (multi)magnon/phonon-assisted electronic resonances driven by temperature shifts. To further explore this possibility, we first probed the electronic structure of BiFeO_3 at high energies, i.e., close to the band edge.

Temperature dependent linear absorption measurements (from $T = 5$ to 730 K) and parameterization analysis were performed on a BiFeO_3 film on DyScO_3 (110). For the series of temperature dependent measurements, the complex index of refraction ($N = n + ik$) were extracted by fitting the experimental ellipsometric spectra to an optical model consisting of a semi-infinite DyScO_3 substrate/100 nm BiFeO_3 film/air ambient structure. Free parameters correspond to the parameterization of the BiFeO_3 dielectric function¹⁹ represented by this film by a Lorentz oscillator, three Tauc-Lorentz oscillator sharing a common Tauc gap, and a constant additive term to ϵ_1 represented by ϵ_∞ .^{20,21} Figure 2(a) shows an example of experimental transmittance spectra at $T = 5 \text{ K}$ for the 100 nm $\text{BiFeO}_3/\text{DyScO}_3$ substrate stack and fit to the corresponding model. It displays an absorption onset at $\sim 2.2 \text{ eV}$, a small shoulder centered at $E_{\text{TL}} \sim 2.5 \text{ eV}$, deriving from onsite d -to- d excitations of the Fe^{3+} ions and two larger features near 3.2 and 4.5 eV that are assigned as charge transfer excitations.^{22,23} All temperature dependent experimental spectra and fits are in good agreement. Figure 2(b) shows the position of the $E_{\text{TL}} \sim 2.5 \text{ eV}$ shoulder extracted from a parameterization of the absorption spectrum as a function of temperature. As observed, it shows singularities at $T_1^* \sim 380 \text{ K}$, $T_5^* \sim 580 \text{ K}$, and T_N , consistent with the previously reported band gap temperature dependence,^{24,25} and the current Raman results. Furthermore, from the results displayed in Fig. 2(b), it can be seen that all the singularities observed in the magnetic Raman response [Fig. 1(e)] occurs within the

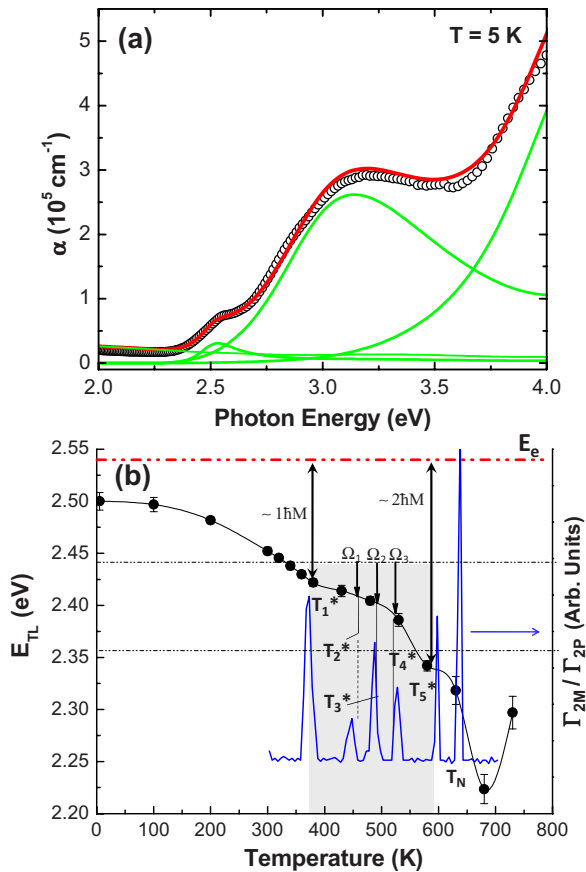


FIG. 2. (Color online) (a) Absorption spectrum obtained for a 100 nm BiFeO₃ film on DyScO₃(110). Solid lines are fits to the parameterized dielectric function at 5 K. (b) (Left axis) Energy position, E_{TL} . Also shown are resonance conditions at T_i^* ($i=1-5$) and T_N involving the Raman excitation wavelength E_{exc} , Tauc-Lorentz energy, E_{TL} , one- and two-magnon and phonons Ω_1 , Ω_2 , and Ω_3 . (Right axis) Integrated intensity ratio between the two-magnon and two-phonon Raman overtones as a function of temperature.

energy range of $E_{TL} \sim 2.43-2.34$ eV. In terms of E_{TL} , the first magnon anomaly at $T_1^* \sim 2.43$ eV is located ~ 0.11 eV below the Raman pump energy ($E_{exc} = 2.54$ eV), while the $T_5^* \sim 2.34$ eV is located ~ 0.2 eV below the Raman pump. These values are close to the expected one-magnon energy ~ 0.1 eV and the observed two-magnon energy ~ 0.19 eV in Fig. 1. Further, the energy separation between T_1^* and the other four transitions in terms of the corresponding shift in E_{TL} are on the 20–50 meV scale. We note that even when a detailed correspondence with specific phonon or magnon modes in BiFeO₃ is presently unwarranted, these energies are clearly on the lattice (phonon and magnon) energy scale.¹⁶ Therefore, the above analysis suggests that the observed Raman enhancements arise from collective interactions involving (multi)magnons, phonons, and electronic states. Indeed, an additional signature for such phonon-magnon interaction at these resonances can be observed in the broad background peak that appears only at these magnon resonances [see Fig. 1(b)]. Such broad features have also been seen in the Raman signal of multiferroic YMnO₃ and are attributed to two-magnon-phonon interactions, where phonons act as intermediate states.²⁶

In summary, we have shown experimental evidence for spin-charge-lattice coupling in multiferroic BiFeO₃. Using a near resonant excitation wavelength (2.54 eV), six Raman enhancements of two-magnon excitations are observed with temperature: one at T_N arising from the antiferromagnetic phase transition and five new ones below T_N , which are shown to be combined resonances involving electronic levels, phonons, and magnon states. The work highlights the sensitivity of multimagnon spectroscopy to spin-charge coupling in multiferroics that has been minimally explored so far and appears to be broadly applicable to other multiferroics and magnetoelectrics.

We acknowledge funding from the National Science Foundation Grant Nos. DMR-0512165, DMR-0507146, DMR-0820404, DMR-0507146, DMR-0820404, and DMR-0602986, DMR-0520513, DMR-0213623, and DMR-0520471 the MSD, BES U.S. Department of Energy under Contract Nos. DE-AC02-05CH11231 and DE-FG02-01ER45885 and the DOE/BES under Contract No. DE-AC02-06CH11357.

¹R. Ramesh and N. A. Spaldin, *Nature Mater.* **6**, 21 (2007).

²S. W. Cheong and M. Mostovoi, *Nature Mater.* **6**, 13 (2007).

³A. Pimenov, A. A. Mukhin, V. D. Travkin, A. M. Balbashov, and A. Loidl, *Nat. Phys.* **2**, 97 (2006).

⁴A. B. Sushkov, R. V. Aguilar, S. W. Cheong, and H. D. Drew, *Phys. Rev. Lett.* **98**, 027202 (2007).

⁵M. Cazayous, Y. Gallais, A. Sacuto, R. de Sousa, D. Lebeugle, and D. Colson, *Phys. Rev. Lett.* **101**, 037601 (2008).

⁶M. K. Shingh, R. Katiyar, and J. F. Scott, *J. Phys.: Condens. Matter* **20**, 252203 (2008).

⁷M. G. Cottam and D. J. Lockwood, *Light Scattering in Magnetic Solids* (Wiley, New York, 1986).

⁸D. Lebeugle, D. Colson, A. Forget, M. Viret, P. Bonville, J. F. Marucco, and S. Fusil, *Phys. Rev. B* **76**, 024116 (2007).

⁹F. Kubel and H. Schmid, *Acta Crystallogr., Sect. B: Struct. Sci.* **46**, 698 (1990).

¹⁰P. Fischer, M. Polomska, I. Sosnowska, and M. Szymanski, *J. Phys. C* **13**, 1931 (1980).

¹¹R. Haumont, J. Kreisel, P. Bouvier, and F. Hippert, *Phys. Rev. B* **73**, 132101 (2006).

¹²T. Zhao, A. Scholl, F. Zavaliche, K. Lee, M. Barry, A. Doran, M. P. Cruz, Y. H. Chu, C. Ederer, N. A. Spaldin, R. R. Das, D. M. Kim, S. H. Baek, C. B. Eom, and R. Ramesh, *Nature Mater.* **5**, 823 (2006).

¹³A. Palewicz, R. Przenioslo, I. Sosnowska, and A. W. Hewat, *Acta Crystallogr., Sect. B: Struct. Sci.* **63**, 537 (2007).

¹⁴M. O. Ramirez, M. Krishnamurthi, S. Denev, A. Kumar, S.-Y. Yang, Y.-H. Chu, E. Saiz, J. Seidel, A. P. Pyatakov, A. Bush, D. Viehland, J. Orenstein, R. Ramesh, and V. Gopalan, *Appl. Phys. Lett.* **95**, 022511 (2008).

¹⁵M. J. Massey, U. Baier, R. Merlin, and W. H. Weber, *Phys. Rev. B* **41**, 7822 (1990).

¹⁶M. K. Singh, H. M. Jang, S. Ryu, and M. Jo, *Appl. Phys. Lett.* **88**, 042907 (2006).

¹⁷P. Baettig, C. Ederer, and N. A. Spaldin, *Phys. Rev. B* **72**, 214105 (2005).

¹⁸The lattice parameters change with temperature, T linearly as $a(X) = 6.73 + 8.7 \times 10^{-5} T(K)$ and $c(X) = 13.81 + 2.21 \times 10^{-4} T(K)$.

¹⁹G. E. Jellison, Jr., *Thin Solid Films* **313**, 33 (1998).

²⁰R. W. Collins and A. S. Ferlauto, in *Handbook of Ellipsometry*, edited by H. G. Tompkins and E. A. Irene, (William Andrew, Norwich, NY, 2005), p. 159–171.

²¹G. E. Jellison, Jr. and F. A. Modine, *Appl. Phys. Lett.* **69**, 371 (1996).

²²S. J. Clark and J. Robertson, *Appl. Phys. Lett.* **90**, 132903 (2007).

²³J. B. Neaton, C. Ederer, U. V. Waghmare, N. A. Spaldin, and K. M. Rabe, *Phys. Rev. B* **71**, 014113 (2005).

²⁴C. Tabares-Munos, J.-P. Rivera, and H. Schmid, *Ferroelectrics* **55**, 235 (1984).

²⁵S. R. Basu, L. W. Martin, Y. H. Chu, M. Gajek, R. Ramesh, R. C. Rai, X. Xu, and J. L. Musfeldt, *Appl. Phys. Lett.* **92**, 091905 (2008).

²⁶J. Takahashi, K. Hagita, K. Kohn, Y. Tanabe, and E. Hanamura, *Phys. Rev. Lett.* **89**, 076404 (2002).